International Endodontic Journal

doi:10.1111/j.1365-2591.2009.01634.x

Laser-activated irrigation within root canals: cleaning efficacy and flow visualization

S. D. de Groot[1]*, B. Verhaagen[2,3]*, M. Versluis[2,3], M.-K. Wu[1], P. R. Wesselink[1] & L. W. M. van der Sluis[1]

[1]Department of Cariology, Endodontology & Pedodontology, Academic Center for Dentistry, Amsterdam; [2]Physics of Fluids Group, Faculty of Science and Technology, University of Twente, Enschede; and [3]Research Institute for Biomedical Technology BMTI, University of Twente, Enschede, The Netherlands

Abstract

de Groot SD, Verhaagen B, Versluis M, Wu M.-K, Wesselink PR, van der Sluis LWM. Laser-activated irrigation within root canals: cleaning efficacy and flow visualization. *International Endodontic Journal*, **42**, 1077–1083, 2009.

Aim To test *ex vivo* the efficiency of laser-activated irrigation in removing dentine debris from the apical part of the root canal and to visualize *in vitro* the fluid dynamics during the activation of the irrigant by laser, using high-speed imaging at a relevant timescale.

Methodology Root canals with a standardized groove in one canal wall filled with dentine debris were irrigated with syringe irrigation, ultrasonically or laser-activated irrigation (LAI) using 2% sodium hypochlorite as irrigant. The quantity of dentine debris after irrigation was determined. Visualization of the fluid dynamics during activation was achieved using a high-speed camera and a glass model.

Results Laser-activated irrigation was significantly more effective in removing dentine debris from the apical part of the root canal than passive ultrasonic irrigation or hand irrigation when the irrigant was activated for 20 s.

Conclusions The *in vitro* recordings suggest that streaming, caused by the collapse of the laser-induced bubble, is the main cleaning mechanism of LAI.

Keywords: irrigation, laser, root canal, ultrasound, visualization.

Received 16 April 2009; accepted 18 August 2009

Introduction

An important procedure during root canal treatment is the irrigation of the root canal. Syringe irrigation is the standard procedure but unfortunately, syringe irrigation is not effective in the apical part of the root canal (Ram 1977, Salzgeber & Brilliant 1977, Abou-Rass & Patonai 1982, Druttman & Stock 1989) and in isthmuses or oval extensions (Lee *et al.* 2004, Burleson *et al.* 2007). Therefore, acoustic and hydrodynamic activation of the irrigant have been developed (Weller *et al.* 1980, Lumley *et al.* 1991, Lussi *et al.* 1993), which have been shown to contribute to the cleaning efficiency (Lumley *et al.* 1991, Lussi *et al.* 1993, Roy *et al.* 1994). The physical mechanisms underlying these cleaning procedures, however, are not well-understood (van der Sluis *et al.* 2007a).

Laser-activated irrigation (LAI) has been introduced as a powerful method for root canal irrigation (Blanken & Verdaasdonk 2007, George & Walsh 2008, George *et al.* 2008). The laser radiation produces transient cavitation in the liquid through optical breakdown by strong absorption of the laser energy (Blanken & Verdaasdonk 2007). LAI can result in smear layer removal from the root canal wall, but also cause extrusion of irrigant through the apex (George & Walsh 2008, George *et al.* 2008). However, the removal of dentine debris from the root canal by LAI has not yet been studied. Furthermore, Blanken & Verdaasdonk (2007) suggested repeating

Correspondence: Bram Verhaagen, MSc, University of Twente, Meander 213, PO Box 217, 7500 AE Enschede, The Netherlands (Tel.: +31 53 489 3084; fax: +31 53 489 8068; e-mail: b.verhaagen@tnw.utwente.nl).

*These two authors should both be listed as primary author, as both contributed equally to this study.

their visualization experiment with a single high-speed camera recording, visualizing a single pulse, to improve the understanding of the cavitation process.

The purpose of this study was to evaluate *ex vivo* the removal of artificially placed dentine debris in standardized root canals by syringe irrigation, passive ultrasonic irrigation (PUI) and LAI. LAI was also visualized *in vitro* using high-speed imaging at a timescale relevant to the cleaning process (μs). The resulting flow is theoretically described using a fluid-dynamical model.

Materials and methods

Dentine debris removal

Maxillary canines with straight root canals were decoronated; the length of the remaining root was 15 mm for all teeth. The roots were then embedded in self-curing acrylic resin (Ostron 100, GC Tokyo, Japan) and then split longitudinally through the canal in mesio-distal direction. To remove the imprint of the root canal, both halves were ground with sandpaper and fixed with four screws (see Fig. 1a). Then, the root canals were prepared by K-files hand instruments (Dentsply Maillefer, Ballaigues, Switzerland) and mechanically driven Race NiTi instruments (FKG Dentaire, La Chaux-de-Fonds, Switzerland), to a length of 15 mm, size 35 and 0.06 taper resulting in a standardized root canal. To verify the standardization of the models, the canal diameter of six randomly chosen models was measured at 2, 6 and 10 mm from the apical end of the canal, using a KS100 Imaging system 3.0 (Carl Zeiss Vision GmbH, Halbermoos, Germany). At 2 mm, the average canal diameter was found to be 0.47 ± 0.02 mm (diameter of the Race NiTi instrument: 0.47 mm); at 6 mm the average canal diameter was 0.71 ± 0.02 (0.71) and at 10 mm the diameter was 0.94 ± 0.02 (0.95). These measured values demonstrate that the root canals were indeed uniform and standardized.

The coronal 3 mm of the canal was enlarged by a no. 23 round bur (Dentsply Maillefer) with a diameter of 2.3 mm, simulating a pulp chamber. A standard

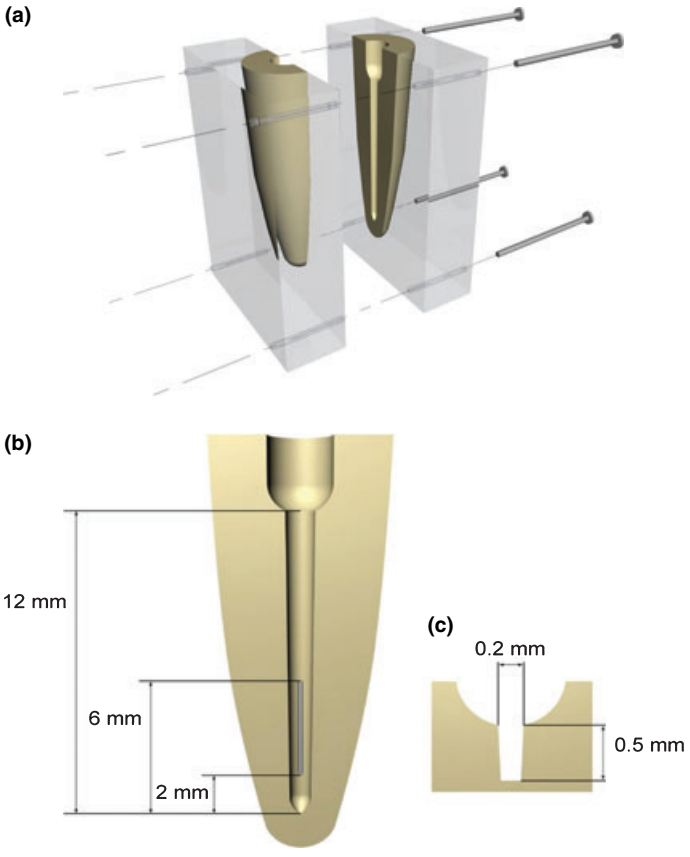

Figure 1 Schematic representations of the standardized root canal model (a), its groove (b), and its cross section (c).

groove of 4 mm in length, 0.5 mm deep and 0.2 mm wide, situated at 2–6 mm from working length, was cut in the wall of one-half of each root canal with an ultrasonically driven tip (Fig. 1b,c) (P5 Booster, Satelec, Acteongroup, Mérignac-cedex, France). The dimension of the groove was comparable with that of an oval extension of a root canal. Each groove was filled with dentine debris mixed with 2% NaOCl to simulate a situation in which dentine debris accumulates in uninstrumented canal extensions (Lee *et al.* 2004). This model was introduced to standardize the root canal anatomy and the amount of dentine debris present in the root canal before the irrigation procedure, in order to increase the reliability of dentine debris removal evaluation. The methodology is sensitive and the data are reproducible (van der Sluis *et al.* 2007b).

Three irrigation protocols were tested. In all groups, the needle, wire and fibre were inserted 1 mm short of the working length and were moved slowly up and down 4 mm in the apical half of the root canal; the activation time was 20 s, the total irrigation time was 50 s and the total irrigant volume was 4 mL. In group 1 ($n = 20$) syringe irrigation with 4 mL of 2% NaOCl solution was performed with a 10 mL syringe and a 30 gauge needle (Navitip, Ultradent, South Jordan, UT, USA). In group 2 ($n = 20$), the 2% NaOCl solution was activated by ultrasound using PUI. A stainless steel noncutting wire (size 20) (Irrisafe, Satelec, Acteongroup) was used, driven by an ultrasonic device (Suprasson Pmax Newtron, Satelec, Acteongroup) at power setting 'blue 4' (frequency 30 KHz, displacement amplitude *ca.* 30 μm according to the manufacturer). Subsequently the canal was flushed with 2 mL of 2% NaOCl solution using a 10 mL syringe and a 30 gauge needle. In group 3 ($n = 20$), the 2% NaOCl solution was activated by laser radiation (KEY2 laser, KaVo Dental GmbH, Biberach, Germany) from an optical fibre laser tip with outer diameter 280 μm and length 30 mm (type Gr. 30 × 28, Kavo Dental GmbH). Calibration by the manufacturer showed that the optical fibre has a reduction factor of 0.36, which results in a fluence of 146 mJ mm^{-2} for a laser pulse energy setting of 100 mJ. The Er:YAG laser emits at a wavelength of 2.94 μm which coincides with the major absorption band of water (Robertson & Williams 1971). A pilot study demonstrated that the optimal settings for dentine debris removal from the root canal are a low power setting of 80 mJ per pulse and a pulse repetition frequency of 15 Hz. Finally, the canal was flushed with 2 mL of 2% NaOCl solution using a 10 mL syringe and a 30 gauge needle.

After irrigation the root canals were dried with paper points. Subsequently, the two halves were separated and the amount of debris in the groove was evaluated. Before and after the irrigation, a digital image was taken of the groove, using a Photomakroskop M400 microscope with a digital camera (Wild, Heerbrugg, Switzerland) at 40× magnification. The quantity of dentine debris in the groove before and after irrigation was scored double blind and independently by three dentists using the following scores: score 0: the groove is empty, score 1: less than half of the groove is filled with dentine debris; score 2: more than half of the groove is filled with dentine debris; score 3: the groove is completely filled with dentine debris. The differences in dentine debris scores between the different groups were analysed by means of the Kruskal–Wallis and Mann–Whitney tests (level of significance $\alpha = 0.05$).

High-speed imaging experiments

An optical setup was constructed in order to visualize the effect of the Er:YAG laser radiation in an artificial root canal containing water or NaOCl. Optical recordings were made at a pulse repetition rate of the Er:YAG laser of 1 Hz and a pulse energy between 80 and 250 mJ per pulse. The laser fibre tip was inserted up to 1 mm from the apical end of a glass root canal model. The canal was 12 mm in length with an apical diameter of 0.35 mm and taper 0.06. Imaging was performed using a high-speed camera (FastCam APX-RS, Photron, Tokyo, Japan), recording at a frame rate of 14 000 frames per second, attached to a microscope with 12× magnification (SZX12, Olympus, Tokyo, Japan). The root canal model was illuminated in bright-field by a continuous wave light source (ILP-1, Olympus).

Results

Dentine debris removal

The debris scores before and after irrigation are presented in Table 1. The difference between the groups was statistically significant (Kruskal–Wallis test, $P < 0.0001$). The debris score in group 3 was significantly lower than group 2 ($P = 0.002$) and group 1 ($P < 0.0001$), and the score in group 2 was significantly lower than group 1 ($P < 0.0001$).

Table 1 Dentine debris score in the groove after the irrigation procedures per group (no. cases and percentage of total; 20 cases in total for each irrigation procedure)

Score:	0 *n* (%)	1 *n* (%)	2 *n* (%)	3 *n* (%)
Syringe irrigation	0	0	4 (20%)	16 (80%)
Ultrasonic irrigation	6 (30%)	8 (40%)	6 (30%)	0
Laser-activated irrigation	16 (80%)	4 (20%)	0	0

Scoring system: 0: the groove is empty; 1: less than half of the groove is filled with debris; 2: more than half of the groove is filled with debris; 3: the complete groove is filled with debris.

High-speed imaging experiments

The high-speed recordings of the laser activity inside the artificial (glass) canal showed that irrigant was vapourized by the laser pulse energy and that a large vapour bubble was created at the fibre tip, similar to that observed previously (Lauterborn 1972). The bubble grew with a velocity of the order of 1 m s^{-1} during the pulse duration (see Fig. 2 and video clips S1 and S2); a higher energy laser pulse corresponded to a longer growth time of the bubble. When the laser pulse ended, the bubble collapsed with a velocity of the order of 1 m s^{-1}. Upon collapse, a shockwave was generated (Holzfuss *et al.* 1998), whose negative-pressure tail caused secondary cavitation in the root canal with a relatively large bubble near the collapse site (which was usually at the apex). The cavitation bubble then collapsed again and this cycle repeated for a number of times, until it was damped out within a few milliseconds (6 ms at 250 mJ per pulse). Smaller bubbles with a typical diameter of 10 μm remain buoyant for a longer time (even up to the next pulse), also at the apical end of the root canal.

The laser-induced bubble grew predominantly in the coronal direction, as there was a confinement at the apex. The depth reached by this bubble depended on the position of the fibre and the laser energy, but never fully extended to the apex. It was observed that when a small bubble was present at the apex, it grew during the collapse phase of the laser-induced bubble and

Figure 2 (Video clips S1 and S2) Visualization of the laser-generated vapor bubble. The laser energy was 60 mJ per pulse in (a) and 250 mJ per pulse in (b). Image sequence is from left to right. The interframe time is 140 μs. Panel *p* in (a) shows a sketch of the setup, with 1) the root canal model, 2) the laser fiber tip (outer diameter 280 μm), 3) the laser-induced cavitation bubble, and 4) a stable cavitation bubble at the apex.

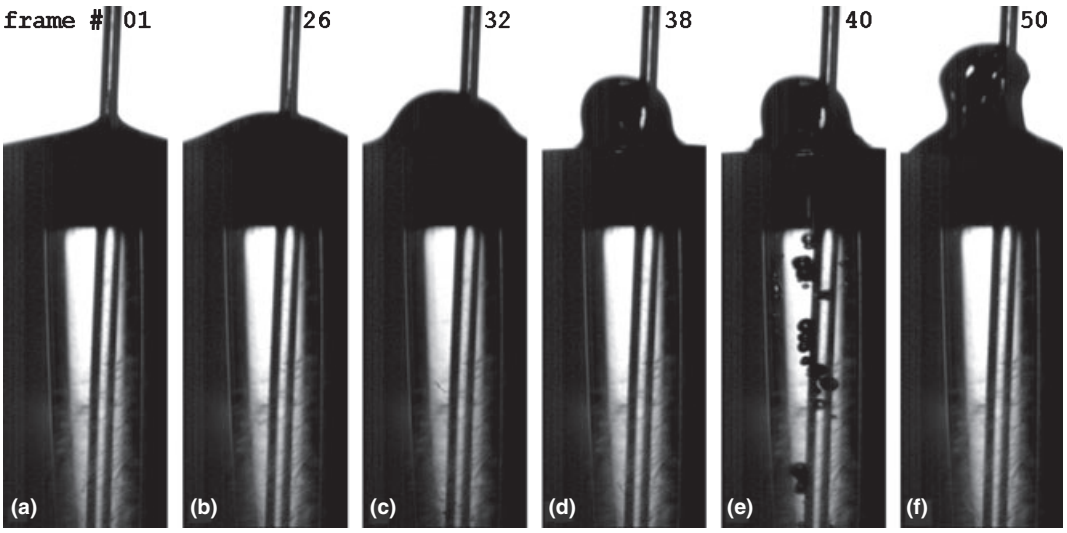

Figure 3 (Video clip S3) Pinch-off at the free surface at the coronal part of the glass root canal model. Secondary cavitation bubbles are formed (in *e*) upon passage of a shockwave generated by the vapor bubble inertial collapse at the laser fiber tip. The frame rate is 14,000 frames/second.

collapsed and renucleated in anti-phase with the laser-induced bubble (Fig. 2a (indicated with the no. 4 in panel *p*), whereas in Fig. 2b this bubble was not present).

It was observed that the laser-induced bubble grew larger when NaOCl was used as an irrigant solution. Consequently, it had a longer collapse time as compared with having water as an irrigant. It was also found that a higher amount of smaller bubbles were present after laser activation when using NaOCl as the irrigant solution.

Because of the impulsive growth of the laser-induced bubble the fluid was pushed outward at the free surface at the coronal part (see Fig. 3 and Video Clip S3). For a laser energy exceeding 120 mJ per pulse it was observed that some fluid was ejected from the root canal, leaving less irrigant in the root canal.

Discussion

The results of the *ex vivo* experiments demonstrate that within the time frame of 20 s, LAI is more effective in removing dentine debris from an artificial groove in the apical part of the root canal than ultrasonically activated (PUI) or syringe-activated irrigation.

The high-speed recordings have shown that vapourization of the irrigant causes a large bubble to grow, which then collapses and renucleates a few times. During this process, secondary cavitation bubbles are formed. The fluid flow associated with such an inertial collapse, combined with acoustic streaming resulting from the oscillations of smaller bubbles, could explain the cleaning efficacy of LAI; however, a more detailed study is required to elucidate the principal cleaning mechanism. The secondary cavitation bubbles can also assist in the cleaning of the root canal wall, as they are excited by the bubble collapse of the consecutive laser pulse. As the flow does not penetrate all the way into the apex, a trapped bubble in the apex (most likely a remainder of previous laser pulses) could assist in the cleaning of the apical part of the root canal.

The irrigant flow in the root canal due to the collapsing laser-induced bubble can be modelled by a flow in concentric annuli for heights above the insertion depth of the fibre. For the typical flow velocity of 1 m s^{-1} (value obtained from the high-speed recordings by measuring the bubble wall displacement between consecutive frames), the Reynolds number $Re = Ud\rho/\mu$ (with U the flow velocity, d the distance between the cylinders, ρ the density of the liquid and μ the dynamic viscosity) for a flow in annuli is of the order of 300. According to Rothfus *et al.* (1950), the transition to turbulence occurs over the range 2100–3700, therefore the flow in this problem is treated as laminar flow.

Rothfus *et al.* (1950) also give the laminar flow velocity distribution for flow in concentric annuli:

$$u(r) = 2u_{av}\frac{\left[r_1^2 - r^2 + \frac{r_2^2 - r_1^2}{\ln\frac{r_2}{r_1}}\ln\frac{r}{r_1}\right]}{r_2^2 + r_1^2 - 2r_m^2} \quad (1)$$

where r_m is the radius of maximum velocity, given by:

$$r_m = \left[\frac{r_2^2 - r_1^2}{2\ln\frac{r_2}{r_1}}\right]^{\frac{1}{2}} \quad (2)$$

Using $\tau = -\mu\frac{\partial u}{\partial r}$ the shear stress for laminar flow in annuli is given by:

$$\tau(r) = -2\mu u_{av}\frac{\left(\frac{r_2^2 - r_1^2}{r} - 2r\ln\frac{r_2}{r_1}\right)}{(r_2^2 + r_1^2)\ln\frac{r_2}{r_1} - r_2^2 + r_1^2} \quad (3)$$

Using standard values for density ρ = 1000 kg m^{-3} and dynamic viscosity $\mu = 1 \times 10^{-3}$ m^2 s^{-1}, and a measured average velocity u_{av} = 5 m s^{-1} and cylinder radii r_1 = 140 μm (inner) and r_2 = 300 μm (outer), the shear stress on the inner wall is 496 N m^{-2} and on the outer wall 436 N m^{-2}. These values are one order of magnitude lower than the shear stress generated by a laser-induced cavitation bubble of radius 0.75 mm next to a single wall, which is reported to generate a shear stress of up to 3.5×10^3 N m^{-2} (Dijkink & Ohl 2008). No quantitative data on the adhesion strength of dental intracanal biofilms to dentine or its failure shear stress is available in the literature.

Figure 4 shows the velocity profile calculated with the theory described above in a tapered canal with a cylinder inserted, assuming an average velocity of 5 m s^{-1} at the fibre tip (taken from experiment). The profile on the left of the inner cylinder is the velocity profile; the profile on the right is the shear stress distribution. The plot clearly shows that on the inner cylinder (the laser fibre) the shear stress is higher than on the outer cylinder (the root canal wall).

The root canal diameter increases with height, therefore the average velocity decreases with height. This results in the shear stress being highest next to the tip of the laser fibre. LAI is therefore expected to be most effective in the region close to the fibre tip, with decreasing efficiency away from the tip.

Using a 27G needle and a volume flow rate of 0.30 mL s^{-1} (Boutsioukis *et al.* 2007) it follows that the typical fluid velocity in syringe irrigation is of the order of 1 m s^{-1} at the needle orifice, which is the same order of magnitude as the flow velocities developed with LAI. Likewise for PUI with $u = \omega\varepsilon_0{}^2/a$ (Ahmad *et al.* 1988; ω = oscillation frequency, ε_0 = oscillation amplitude and a = file radius) a typical fluid velocity of the order of 1 m s^{-1} was found. One possible explanation for the improvement in cleaning efficacy with LAI is the impulsive nature of the laser-generated bubble dynamics. Because of the pulsations the fluid becomes accelerated at every pulse and the acceleration gives rise to inertial forces, whereas a steady streaming as in syringe irrigation and PUI only exerts viscous stress. This would also explain why the irrigation duration is an important factor and why a high pulse repetition rate of the laser is more efficient than a lower one, as found in the pilot-study.

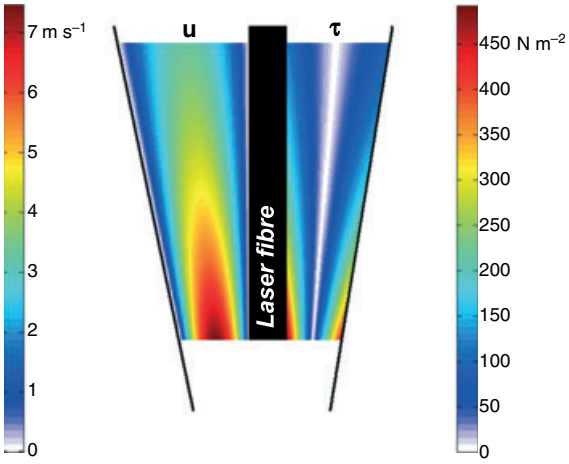

Figure 4 Average velocity profile (left) and sheer stress distribution (right) between two concentric cylinders of which the outer cylinder represents the tapered root canal wall. The average velocity at the laser fiber tip is set at 5 m s^{-1}. The region below the laser fiber tip is intentionally left blank, as details of the streaming pattern in the apical part are missing and are part of a future study.

Previous studies have shown side-effects caused by the use of these types of lasers in the root canal. Carbonization of the root canal and cracks were observed when laser tips were used in the root canal (Matsuoka *et al.* 2005). Kimura *et al.* (2002) have shown a temperature increase of the root canal wall of 3–6 °C. The current study did not monitor these side-effects, because the aim of this study was clarification of the fluid mechanical working mechanisms.

Conclusion

Laser-activated irrigation was more effective in removing the artificially placed dentine debris from the root canal than syringe irrigation or PUI when the irrigant was activated for 20 s.

Acknowledgements

We thank Gert-Wim Bruggert for technical support and Gerrit J. de Bruin for valuable discussions on the theoretical approach of the fluid flow in tapered canals.

References

Abou-Rass M, Patonai FJ (1982) The effects of decreasing surface tension on the flow of irrigating solutions in narrow root canals. *Oral Surgery, Oral Medicine, Oral Pathology* **53**, 524–6.

Ahmad M, Pitt Ford TR, Crum LA, Walton AJ (1988) Ultrasonic debridement of root canals: acoustic streaming and its relevance. *Journal of Endodontics* **14**, 486–93.

Blanken JW, Verdaasdonk RM (2007) Cavitation as a working mechanism of the Er,Cr:YSGG Laser in endodontics: a visualization study. *Journal of Oral Laser Applications* **7**, 97–106.

Boutsioukis C, Lambrianidis T, Kastrinakis E, Bekiaroglou P (2007) Measurement of pressure and flow rates during irrigation of a root canal *ex vivo* with three endodontic needles. *International Endodontic Journal* **40**, 504–13.

Burleson A, Nusstein J, Reader A, Beck M (2007) The *in vivo* evaluation of hand/rotary/ultrasound instrumentation in necrotic, human mandibular molars. *Journal of Endodontics* **33**, 782–7.

Dijkink R, Ohl C-D (2008) Measurement of cavitation induced wall shear stress. *Applied Physics Letters* **93**, 2541071–3.

Druttman AC, Stock CJ (1989) An *in vitro* comparison of ultrasonic and conventional methods of irrigant replacement. *International Endodontic Journal* **22**, 174–8.

George R, Walsh LJ (2008) Apical extrusion of root canal irrigants when using Er:YAG and Er,Cr:YSGG lasers with optical fibers: an *in vitro* dye study. *Journal of Endodontics* **34**, 706–8.

George R, Meyers IA, Walsh LJ (2008) Laser activation of endodontic irrigants with improved conical laser fiber tips for removing smear layer in the apical third of the root canal. *Journal of Endodontics* **34**, 1524–7.

Holzfuss J, Rüggeberg M, Billo A (1998) Shock wave emissions of a sonoluminescing bubble. *Physical Review Letters* **81**, 5434–7.

Kimura Y, Yonaga K, Yokoyama K, Kinoshita J, Ogata Y, Matsumoto K (2002) Root surface temperature increase during Er:YAG laser irradiation of root canals. *Journal of Endodontics* **28**, 76–8.

Lauterborn W (1972) High-speed photography of laser-induced breakdown in liquids. *Applied Physics* **21**, 27–9.

Lee S-J, Wu M-K, Wesselink PR (2004) The efficacy of ultrasonic irrigation to remove artificially placed dentin debris from different sized simulated plastic root canals. *International Endododontic Journal* **37**, 607–12.

Lumley PJ, Walmsley AD, Laird WRE (1991) Streaming patterns around endosonic files. *International Endodontic Journal* **24**, 290–7.

Lussi A, Nussbächer U, Grosrey J (1993) A novel noninstrumented technique for cleansing the root canal system. *Journal of Endodontics* **19**, 549–53.

Matsuoka E, Jayawardena JA, Matsumoto K (2005) A morphological study on root canal preparation using Erbium, Chromium:YSGG laser. *Journal of Oral Laser Applications* **5**, 17–21.

Ram Z (1977) Effectiviness of root canal irrigation. *Oral Surgery, Oral Medicine, Oral Pathology* **44**, 306–11.

Robertson CW, Williams D (1971) Lambert absorption coefficients of water in the infrared. *Journal of the Optical Society of America* **61**, 1316–20.

Rothfus RR, Monrad CC, Senecal VE (1950) Velocity distribution and fluid friction in smooth concentric annuli. *Industrial & Engineering Chemistry* **42**, 2511–20.

Roy RA, Ahmad M, Crum LA (1994) Physical mechanisms governing the hydrodynamic response of an oscillating ultrasonic file. *International Endodontic Journal* **27**, 197–207.

Salzgeber RM, Brilliant JD (1977) An *in vitro* evaluation of the penetration of an irrigating solution in root canals. *Journal of Endodontics* **3**, 394–8.

van der Sluis LMW, Wu M-K, Versluis M, Wesselink PR (2007a) Passive ultrasonic irrigation of the root canal: a review of the literature. *International Endodontic Journal* **40**, 415–26.

van der Sluis LWM, Wu MK, Wesselink PR (2007b) The evaluation of removal of $Ca(OH)_2$ from an artificial standardized groove in the apical root canal using different irrigation methodologies. *Internaional Endodontic Journal* **40**, 52–7.

Weller RN, Brady JN, Bernier WE (1980) Efficacy of ultrasonic cleaning. *Journal of Endodontics* **6**, 740–3.

Supporting Information

Additional supporting information may be found in the online version of this article.

Video Clip S1. Visualization at the apex of the root canal, laser intensity 60 mJ/pulse (*apex_energy60mj.wmv*).

Video Clip S2. Visualization at the apex of the root canal, laser intensity 250 mJ/pulse (*apex_energy250mj.wmv*).

Video Clip S3. Visualization at the corona of the root canal, laser intensity 250 mJ/pulse (*corona_energy250mj.wmv*)

Please note: Wiley-Blackwell is not responsible for the content or functionality of any supporting information supplied by the authors. Any queries (other than missing material) should be directed to the corresponding author for the article.